

# Heat and mass transfer on MHD flow of Non-Newtonian fluid over an infinite vertical porous plate

K.Raghunath<sup>1\*</sup>, R.Siva Prasad<sup>2</sup>, and G.S.S.Raju<sup>3</sup>

<sup>1</sup>Research Scholar, JNTU College of Engineering, Anantapur, Andhra Pradesh, India.

<sup>2</sup>Professor, Department of Mathematics, S.K.University, Anantapur, Andhra Pradesh, India.

<sup>3</sup>Professor, Department of Mathematics, JNTUA College, Pulivendula, Andhra Pradesh, India.

## Abstract

We have considered the boundary-layer flow of a heat-absorbing MHD non-Newtonian fluid along a semi-infinite vertical porous moving plate in the presence of thermal buoyancy effect. The dimensionless governing equations are solved analytically using two-term harmonic and non-harmonic functions. Computational analysis of the results is presented with a view to reveal for the velocity, temperature and concentration profiles within the boundary layer. The Skin friction, Nusselt number and Sherwood number are also examined with the reference to governing parameters.

**Keywords:** MHD flows, non-Newtonian flow, porous medium and unsteady flows

## INTRODUCTION

The magnetohydrodynamic (MHD) flows of viscous incompressible fluid through porous medium over an infinite porous plate have been investigated rigorously by many researchers because of its wide application in different fields. The phenomenon of flows through porous medium has been a subject of interest of many researchers because of its wide range of application in different fields such as petroleum engineering, chemical engineering etc. In petroleum engineering, it is dealt with the movement of natural gas and oil through reservoirs. Further, the study on underground water resources, seepage of water in river bed is also related to the flow through porous medium. Soundalgekar and Puri [1] investigated on the flow of an elastic-viscous fluid past an infinite plate with variable suction. Shen, Tan, Zhao and Masuoka [2] studied the Rayleigh-Stokes problem for a heated generalized second grade fluid with fractional derivative model. Varshney [3] studied fluctuating flow of viscous fluid through a porous medium bounded by a porous plate. In his work, he has used Lighthill's method in finding the solution of the field equation and shows that the results obtained reduce those of Messiha [5]. Lighthill [4] initiated the work on fluctuating flows. He studied the response of laminar skin friction and heat transfer to fluctuations in the stream velocity. An important class of two dimensional time dependent flow problems dealing with the response of the boundary layer to unsteady fluctuations about a mean value has been studied by him. Messiha [5] investigated laminar

boundary layer in oscillating flow along an infinite flat plate with variable suction. Stuart [6] studied a solution of the Navier-Stokes and energy equations illustrating the response of skin friction and temperature of an infinite plate thermometer to fluctuations in the stream velocity. Gholizadeh [7] discussed MHD oscillatory flow past a vertical porous plate through porous medium in the presence of thermal and mass diffusion with constant heat source. Moniem and Hassanin [8] investigated solution of MHD flow past a vertical porous plate through a porous medium under oscillatory suction. Venkateswarlu, Reddy and Lakshmi [9] studied unsteady MHD flow of a viscous fluid past a vertical porous plate under oscillatory suction velocity. Raghunath, Siva Prasad and GSS Raju [10] discussed Heat and mass transfer on Unsteady MHD flow of a second grade fluid through porous medium between two vertical plates. Soundalgekar and Takhar [12] discussed MHD oscillatory flow past a semi infinite plate. Recently, Krishna et al [13-15] discussed the MHD flows of an incompressible and electrically conducting fluid in planar channel. Recently K Raghunath and Krishna [16] discussed Heat and Mass Transfer on Unsteady MHD Flow of a Visco-Elastic Fluid Past an Infinite Vertical Oscillating Porous Plate.

Motivated by the above studies, in this paper we have considered MHD flow of non-Newtonian (Rivlin-Ericksen) fluid past a semi-infinite moving porous plate.

## FORMULATION AND SOLUTION OF THE PROBLEM

We consider the MHD flow of an electrically conducting and heat absorbing Non-Newtonian fluid (Rivlin-Ericksen type) over a semi-infinite vertical permeable moving plate embedded in a porous medium with a uniform transverse magnetic field (Fig.1). It is assumed that there is no applied voltage which implies the absence of a electrical field the transversely applied magnetic field and magnetic Reynolds number are assumed to be very small to that the induced magnetic field and the hall effects are negligible. A consequence of the small magnetic Reynolds number is a the uncoupling of the Navier-stokes equations from Maxwell's equations the governing equations for this investigation are based on the balances of mass, linear momentum made above,

these equations can be written in Cartesian frame of reference as follows:

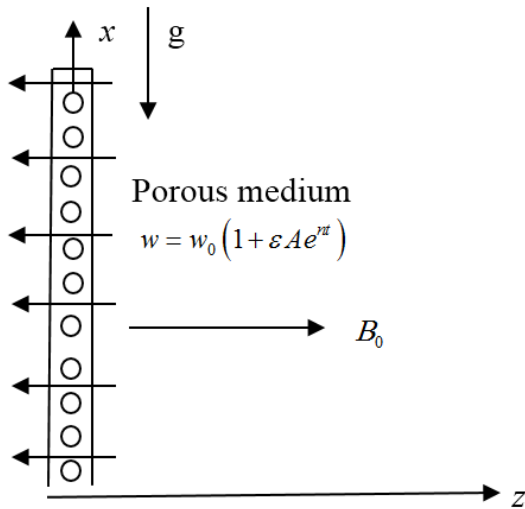


Figure 1. Physical configuration of the Problem.

$$\frac{\partial w}{\partial z} = 0 \quad (1)$$

$$\frac{\partial u}{\partial t} + w \frac{\partial u}{\partial z} = -\frac{1}{\rho} \frac{\partial p}{\partial x} + \frac{\partial^2 u}{\partial z^2} - \beta_1 \left( \frac{\partial^3 u}{\partial t \partial z^2} + v \frac{\partial^3 u}{\partial z^3} \right) - \frac{\sigma B_0^2}{\rho} u - \frac{v}{k} u + \beta_T (T - T_\infty) + \beta_C (C - C_\infty) \quad (2)$$

$$\frac{\partial v}{\partial t} + w \frac{\partial v}{\partial z} = -\frac{1}{\rho} \frac{\partial p}{\partial y} + v \frac{\partial^2 v}{\partial z^2} - \beta_1 \left( \frac{\partial^3 v}{\partial z^2 \partial t} + \frac{\partial^3 v}{\partial z^3} \right) - \frac{\sigma B_0^2}{\rho} v - \frac{v}{k} v \quad (3)$$

$$\frac{\partial T}{\partial t} + w \frac{\partial T}{\partial z} = \alpha \frac{\partial^2 T}{\partial z^2} - \frac{Q_0}{\rho C_p} (T - T_\infty) \quad (4)$$

$$\frac{\partial C}{\partial t} = D \frac{\partial^2 C}{\partial z^2} \quad (5)$$

Where  $x$ ,  $z$  and  $t$  are the dimensional distance along and perpendicular to the plate and dimensional time, respectively  $u$  and  $v$  are the components of dimensional velocities along  $x$  and  $z$  directions respectively  $\rho$  is the fluid density,  $\nu$  is the kinematic velocity,  $C_p$  is the specific heat at constant pressure,  $\sigma$  is the fluid electrical conductivity,  $B_0$  is the magnetic induction,  $k$  is the permeability of the porous medium.  $T$  is the dimensional temperature,  $Q_0$  is the dimensional heat observation co-efficient,  $\alpha$  is the thermal diffusivity,  $g$  is the gravitational acceleration and  $\beta_T$  is the coefficient of volumetric thermal expansion,  $\beta_C$  is volumetric expansion coefficient for concentration and  $\beta_1$  is the kinematic viscoelasticity.

The magnetic and viscous dissipations are neglected in this study. It is assumed that the permeable plate moves with a constant velocity in the direction of fluid flow and the free

steam velocity follows the exponentially increasing small perturbation law. In addition, it is assumed that the temperature at the wall as well as the suction velocity is exponentially varying with time. Under then assumptions the appropriate conditions for the velocity, temperature fields are

$$u = U_p, v = 0, T = T_w + \varepsilon(T_w - T_\infty)e^{nt}, C = C_w + \varepsilon(C_w - C_\infty)e^{nt} \text{ at } z = 0 \quad (5)$$

$$u \rightarrow U_\infty, v \rightarrow 0 = u_0(1 + \varepsilon e^{nt}), T \rightarrow T_\infty, C \rightarrow C_\infty, \text{ as } z \rightarrow \infty \quad (6)$$

Where  $U_p$ ,  $T_w$  are the wall dimensional velocity temperature, respectively  $U_\infty, T_\infty$  are the free steam dimensional velocity, temperature respectively,  $u_0$  and  $\eta$  are constants.

It is clear from equation (1) that the suction velocity at the plate surface is a function of time only assuming that it takes the following exponential form

$$w = -w_0(1 + \varepsilon A e^{nt}) \quad (7)$$

Combining equations (2) and (3), let

$q = u + iv$  and  $\xi = x - iy$ , we obtain,

$$\frac{\partial q}{\partial t} + w \frac{\partial q}{\partial z} = -\frac{1}{\rho} \frac{\partial p}{\partial \xi} + v \frac{\partial^2 q}{\partial z^2} - \beta_1 \left( \frac{\partial^3 q}{\partial z^2 \partial t} + v \frac{\partial^3 q}{\partial z^3} \right) - \left( \frac{\sigma B_0^2}{\rho} + \frac{v}{k} \right) q + g\beta_T (T - T_\infty) + g\beta_C (C - C_\infty) \quad (8)$$

Where  $A$  is a real positive constants,  $\varepsilon$  and  $\varepsilon A$  are small less than unity, and  $w_0$  is a scale of suction velocity which has non-zero positive constant outside the boundary layer equation (2) gives

$$-\frac{1}{\rho} \frac{\partial p}{\partial \xi} = \frac{\partial U_\infty}{\partial t} + \frac{v}{k} U_\infty + \frac{\sigma}{\rho} B_0^2 U_\infty \quad (9)$$

We introduced the following non-dimensional variables

$$u^* = \frac{u}{U_0}, v^* = \frac{v}{w_0}, z^* = \frac{w_0 z}{\nu}, U_\infty^* = \frac{U_\infty}{U_0}, U_p^* = \frac{u_p}{U_0}, t^* = \frac{t w_0^2}{\nu}, \theta = \frac{T - T_\infty}{T_w - T_\infty}, \phi = \frac{C - C_\infty}{C_w - C_\infty}$$

Making use of non-dimensional variables the governing equations reduces to (Dropping asterisks)

$$\frac{\partial q}{\partial t} - (1 + \varepsilon A e^{nt}) \frac{\partial q}{\partial z} = \frac{\partial U_\infty}{\partial t} + \frac{\partial^2 q}{\partial z^2} + Gr\theta + Gm\phi + N(U_\infty - q) - Rm \frac{\partial^3 u}{\partial t \partial z^2} - (1 + \varepsilon A e^{nt}) \frac{\partial^3 q}{\partial z^3} \quad (10)$$

$$\frac{\partial \theta}{\partial t} - (1 + \varepsilon A e^{nt}) \frac{\partial \theta}{\partial z} = \frac{1}{Pr} \frac{\partial^2 \theta}{\partial z^2} - Q\theta \quad (11)$$

$$\frac{\partial \phi}{\partial t} - (1 + \varepsilon A e^{nt}) \frac{\partial \phi}{\partial z} = \frac{1}{Sc} \frac{\partial^2 \phi}{\partial z^2} \quad (12)$$

Where,  $K = \frac{k w_0}{\nu^2}$  is the permeability of the porous medium,  $Pr = \frac{\nu \rho C_p}{k}$  is the prandtl number,  $M^2 = \frac{\sigma B_0^2 \nu}{\rho w_0^2}$  is the magnetic field parameter,  $Gr = \frac{\nu \beta_T g (T_\infty - T_0)}{w_0^3}$  is the grashof number,  $Sc = \frac{\nu}{D}$  is

the Schmist number,  $Rm = \frac{\beta_1 w_0^2}{\nu^2}$  is the dimensionless form

visco-elasticity parameter of the Rivlin-Ericksen Fluid.

The dimensionless form the boundary conditions equations (5) and (6) become

$$q = U_p, \theta = 1 + \varepsilon e^{mz}, \phi = 1 + \varepsilon e^{mz}, U = 1 + \varepsilon e^{mz} \text{ at } z = 0$$

$$q \rightarrow U_\infty, \theta = 0, \phi \rightarrow 0, U \rightarrow 0 \text{ at } z \rightarrow \infty$$

(13)

Equation (10) and (11) represent a set of partial differential equations that cannot be solved in closed form however if can be reduced to a set off ordinary differential equations in dimensionless fom that can be solved analytically this can be done representing the velocity and temperature as,

$$q = q_0(z) + \varepsilon e^{mz} q_1(z) + O(\varepsilon^2) \quad (14)$$

$$\theta = \theta_0(z) + \varepsilon e^{mz} \theta_1(z) + O(\varepsilon^2) \quad (15)$$

$$\phi = \phi_0(z) + \varepsilon e^{mz} \phi_1(z) + O(\varepsilon^2) \quad (16)$$

Substituting the equations (14), (15) and (16) into equation (10), (11) and(12), equating the harmonic and non-harmonic terms, the neglecting and higher order terms of  $O(\varepsilon^2)$ , one obtains the following pairs of equations  $(q_0, \theta_0, \phi_0)$  and  $(q_1, \theta_1, \phi_1)$ ,

$$Rm \frac{d^3 q_0}{dz^3} + \frac{d^2 q_0}{dz^2} + \frac{dq_0}{dz} - Nq_0 = -Gr\theta_0 - N \quad (17)$$

$$Rm \frac{d^3 q_1}{dz^3} + (1-nRm) \frac{d^2 q_1}{dz^2} + \frac{dq_1}{dz} - Nq_1 - nq_1 = -n - Gr\theta_1 - N - RmA \frac{d^3 q_0}{dz^3} - A \frac{dq_0}{dz} \quad (18)$$

$$\frac{d^2 \theta_0}{dz^2} + Pr \frac{d\theta_0}{dz} - QPr\theta_0 = 0 \quad (19)$$

$$\frac{d^2 \theta_1}{dz^2} + Pr \frac{d\theta_1}{dz} - nPr\theta_1 - QPr\theta_1 = -APr \frac{d\theta_0}{dz} \quad (20)$$

$$\frac{d^2 \phi_0}{dz^2} + Sc \frac{d\phi_0}{dz} = 0 \quad (21)$$

$$\frac{d^2 \phi_1}{dz^2} + Sc \frac{d\phi_1}{dz} - nSc\theta_1 = -ASc \frac{d\theta_0}{dz} \quad (22)$$

The corresponding boundary conditions can be written as

$$q_0 = U_p, q_1 = 0, \theta_0 = 1, \theta_1 = 1, \phi_0 = 1, \phi_1 = 1 \text{ at } z = 0 \quad (23)$$

$$q_0 = 1, q_1 = 1, \theta_0 \rightarrow 0, \theta_1 \rightarrow 0, \phi_0 \rightarrow 0, \phi_1 \rightarrow 0 \text{ at } z \rightarrow \infty \quad (24)$$

Without going into detail, the solution of equation (15)-(18) subject to conditions (23) and (24) can be show to be

$$q_0 = e^{-mz} \quad (19)$$

$$q_1 = a_2 e^{-m_3 z} + a_1 e^{-m_1 z} \quad (20)$$

Equations (15) an (16) are third degree order differential equations when  $Rm \neq 0$  and we have two boundary conditions so we follows bears and Walter's as

$$q_0 = q_{01} + Rmq_{02} + O(Rm^2) \quad (21)$$

$$q_1 = q_{11} + Rmq_{12} + O(Rm^2) \quad (22)$$

Substituting equations (22) and (20) into (15) and (16), equiating different powers of  $Rm$  and neglecting  $O(Rm^2)$  are,

$$\frac{d^2 q_{01}}{dz^2} + \frac{dq_{01}}{dz} - Nq_{01} = -Gre^{-mz} - Gme^{-mz} - N \quad (25)$$

$$\frac{d^3 q_{01}}{dz^3} + \frac{d^2 q_{02}}{dz^2} + \frac{dq_{02}}{dz} - Nq_{02} = 0 \quad (26)$$

$$\frac{d^2 q_{11}}{dz^2} + \frac{dq_{11}}{dz} - (n+N)q_{11} = -n - Gr(a_1 e^{-mz} + a_2 e^{-m_3 z}) - Gm(b_1 e^{-mz} + b_2 e^{-m_3 z}) - N - A \frac{dq_{01}}{dz} \quad (27)$$

$$\frac{d^3 q_{11}}{dz^3} + \frac{d^2 q_{12}}{dz^2} - n \frac{d^2 q_{11}}{dz^2} + \frac{dq_{12}}{dz} - (n+N)q_{12} = -A \frac{d^3 q_{01}}{dz^3} - A \frac{dq_{02}}{dz} \quad (28)$$

The corresponding boundary conditions are

$$q_{01} = u_p, q_{02} = 0, q_{11} = 0, q_{12} = 0 \text{ at } z = 0$$

$$q_{01} = 1, q_{02} = 0, q_{11} = 1, q_{12} = 0, \text{ as } z \rightarrow \infty \quad (29)$$

We get zeroth order and first order solutions of  $Rm$

$$q_{01} = a_4 e^{-m_6 z} + a_3 e^{-m_5 z} + b_4 e^{-m_6 z} + b_3 e^{-n_1 z} + 1 \quad (30)$$

$$q_{02} = a_7 e^{-m_8 z} + a_5 e^{-m_6 z} + b_7 e^{-m_8 z} + b_5 e^{-m_6 z} + a_6 e^{-m_1 z} + b_6 e^{-n_1 z} \quad (31)$$

$$q_{11} = -a_{16} e^{-m_{10} z} + a_9 e^{-m_3 z} + a_{15} e^{-m_1 z} + b_3 e^{-n_3 z} + b_{10} e^{-n_1 z} + a_{12} e^{-m_6 z} + a_{14} \quad (32)$$

$$q_{12} = -a_{27} e^{-m_{12} z} + a_{22} e^{-m_6 z} + a_{23} e^{-m_1 z} + a_{24} e^{-m_3 z} + a_{25} e^{-m_{10} z} + a_{26} e^{-m_3 z} \quad (33)$$

In view of the above solutions, the velocity and temperature distributions in the boundary layer become

$$q(z, t) = q_0(z) + \varepsilon e^{nt} q_1(z)$$

$$\begin{aligned} &= \left[ (a_4 e^{-m_4 z} + a_3 e^{-m_2 z} + b_4 e^{-m_4 z} + b_3 e^{-n_2 z} + 1) + \right. \\ &Rm \left( a_7 e^{-m_8 z} + a_5 e^{-m_6 z} + b_7 e^{-m_8 z} + b_5 e^{-m_6 z} + a_6 e^{-m_1 z} + b_6 e^{-n_1 z} \right) \\ &+ \varepsilon e^{nt} \left[ (-a_{16} e^{-m_{10} z} + a_9 e^{-m_3 z} + a_{15} e^{-m_1 z} + b_8 e^{-n_3 z} + b_{12} e^{-n_1 z} + a_{12} e^{-m_6 z} + a_{14}) \right. \\ &\left. + Rm \left( -a_{27} e^{-m_{12} z} + a_{22} e^{-m_6 z} + a_{23} e^{-m_1 z} + b_{16} e^{-n_3 z} + a_{24} e^{-m_3 z} + a_{25} e^{-m_{10} z} + a_{26} e^{-m_3 z} + b_{17} e^{-n_3 z} \right) \right] \end{aligned}$$

$$\theta(z, t) = \theta_0(z) + \varepsilon e^{nt} \theta_1(z) \quad (30)$$

$$= e^{-m_1 z} + \varepsilon e^{nt} (a_2 e^{-m_3 z} + a_1 e^{-m_1 z}) \quad (31)$$

$$\phi(z, t) = \phi_0(z) + \varepsilon e^{nt} \phi_1(z) \quad (30)$$

$$= e^{-n_1 z} + \varepsilon e^{nt} (b_2 e^{-n_3 z} + b_1 e^{-n_1 z}) \quad (31)$$

The skin friction co-efficient, Nusselt number and Sherwood number are important physical parameters for this type of boundary layer flow. These parameters can be defined and determined as follows.

$$\tau = \left( \frac{\partial q}{\partial z} \right)_{z=0} = (a_{28} + Rma_{29}) + \varepsilon e^{nt} (a_{30} + Rma_{31}) \quad (32)$$

$$Nu = \left( \frac{\partial \theta}{\partial z} \right)_{z=0} = a_{32} + \varepsilon e^{nt} (a_{33}) \quad (33)$$

$$Sh = \left( \frac{\partial \phi}{\partial z} \right)_{z=0} = a_{33} + \varepsilon e^{nt} (a_{35}) \quad (34)$$

## RESULTS AND DISCUSSION

In order to get physical insight into the problem, the effects of various parameters encountered in the equations of the problem are analyzed on velocity and temperature fields with the help of figures (2-11). We have also analyzed the effects of these physical parameters on skin friction coefficient and Nusselt number and are mentioned in the tables (1-2).

We noticed that, the velocity component  $u$  and  $v$  reduces with increasing the intensity of the magnetic field or Hartmann number  $M$ . The similar behaviour is observed for the resultant velocity (Figs. 2). It is obvious that the effect of increasing

values of the magnetic field parameter  $M$  results in a decreasing velocity components  $u$  and  $v$  across the boundary layer. Figs. (3) depicts the effect of permeability of the porous medium parameter ( $K$ ) on velocity distribution profiles for  $u$  and  $v$  and it is obvious that as permeability parameter ( $K$ ) increases, the velocity components for  $u$  and  $v$  increases along the boundary layer thickness which is expected since when the holes of porous medium become larger, the resistive of the medium may be neglected. Similar behaviour is observed with increasing permeability parameter  $K$  for the resultant velocity. Figs. 5 illustrate the variation in velocity components  $u$  and  $v$  with span wise coordinate  $n$  for several values of  $Rm$ . We observed that both  $u$  reduces and  $v$  increases with increasing visco-elastic fluid parameter of the Rivlin-Ericksen fluid  $Rm$ . It was found that an increase in  $Rm$  leads to a decrease in the resultant velocity distribution across the boundary layer. Figs. (5) illustrate the velocity profiles for  $u$  and  $v$  for different values of the Grashof number  $Gr$ . It can be seen that an increase in  $Gr$  leads to a rise in velocity  $u$  and  $v$  profiles. The resultant velocity is also enhances throughout the fluid region with increasing the thermal Grashof number  $Gr$ . We noticed that from the Figs. (6), the magnitude of the velocity component  $u$  reduces and  $v$  enhances with increasing Suction parameter  $A$  throughout the fluid region. The resultant velocity is reduces with increasing Suction parameter  $A$ . Figs. (7) presents the velocity distribution profiles for different values of the Prandtl number ( $Pr$ ). The results show that the effect of increasing values of the prandtl number results in an increase in  $u$  and in a decrease in the velocity component  $v$ . The resultant velocity is also reduces with Prandtl number  $Pr$ . Figs. (8) shows the velocity profiles for  $u$  and  $v$  for different values of dimensionless heat absorption coefficient  $Q$ . Clearly as  $Q$  increase the pack values of velocity components  $u$  increase and  $v$  tends to decrease. The resultant velocity reduces with increasing heat absorption coefficient  $Q$ , physically the presence of heat absorption coefficient has the tendency to reduce the fluid temperature. This causes the thermal buoyancy effects to decrease resulting in a net reduction in the fluid velocity. The Figs. (9) shows the velocity profiles for  $u$  and  $v$  against span wise direction for different values of the scalar constant  $\varepsilon$ . It was found that an increase in the value of  $\varepsilon$  leads to an increase in the resultant velocity distribution across the boundary layer. The velocity component  $u$  diminishes first and then experiences enhancement and where as  $v$  increases with increasing the scalar constant  $\varepsilon$ . Finally, Figs. (10) depicts the effect of the frequency of oscillation  $n$  on the velocity distribution. The primary velocity component  $u$  and secondary velocity  $v$  reduce with increasing the frequency of oscillation  $n$ . The resultant velocity reduces with increasing the frequency of oscillation throughout the fluid medium.

We noticed that from the Figs. 11, the temperature reduces with increasing Prandtl number  $Pr$  or the frequency of oscillation  $n$  or suction velocity  $A$  or heat absorption coefficient  $Q$ . The result display that an increase in the value of  $Q$  results in decrease in the temperature profiles as expected. The temperature profiles with span wise coordinate  $n$  for various scalar constant  $\varepsilon$ . The numerical results show that the effect of increase value of  $\varepsilon$  results in an increase

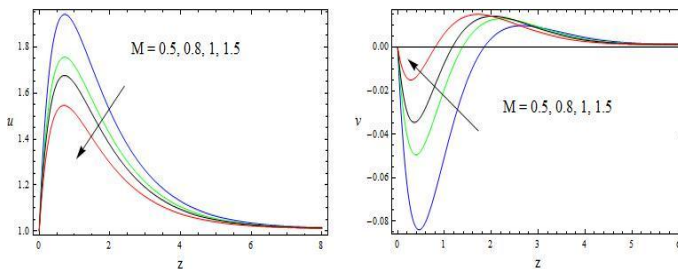
thermal boundary layer thickness and more uniform temperature distribution across the boundary layer. Similar behaviour is observed in entire fluid region with increasing time.

We noticed from the Figs. 12, the temperature reduces with increasing Schmidt number  $Sc$  or the frequency of oscillation  $n$  or suction velocity  $A$ . The Concentration profiles with span wise coordinate  $n$  for various scalar constant  $\mathcal{E}$ . The numerical results show that the effect of increase value of  $\mathcal{E}$  results in an increase concentration boundary layer thickness and more uniform concentration distribution across the boundary layer.

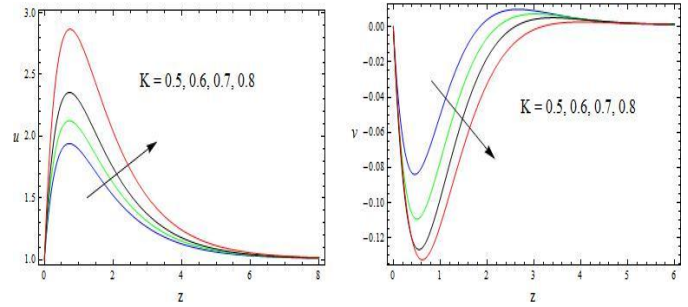
We have also shown Table (1) of the surface skin friction coefficient against some parameters. The stress components  $\tau_x$  and the magnitude of  $\tau_y$  are reduces with increasing the intensity of the magnetic field  $M$ , Schmidt number  $Sc$  or the suction velocity  $A$ . The reversal behaviour is observed throughout the region with increasing Grashof number  $Gr$  or heat absorption coefficient  $Q$  or scalar constant  $\mathcal{E}$ , because an increase in  $Gr$  influences the buoyancy that results in skin friction. The stress component  $\tau_x$  enhances and the magnitude of  $\tau_y$  reduces with increasing permeability parameter  $K$ , where as  $\tau_x$  decreases and the magnitude of  $\tau_y$  boost up with increasing visco-elastic fluid parameter of the Rivlin-Ericksen fluid  $Rm$  or Prandtl number  $Pr$  or frequency of oscillation  $n$ .

The rate of heat transfer ( $Nu$ ) is shown in the Table (2) with reference to all governing parameters. The magnitude of the Nusselt number rise up throughout the fluid region with increasing scalar constant  $\mathcal{E}$ , suction velocity  $A$ , Prandtl number  $Pr$ , heat absorption parameter  $Q$  and the frequency of oscillation  $n$ .

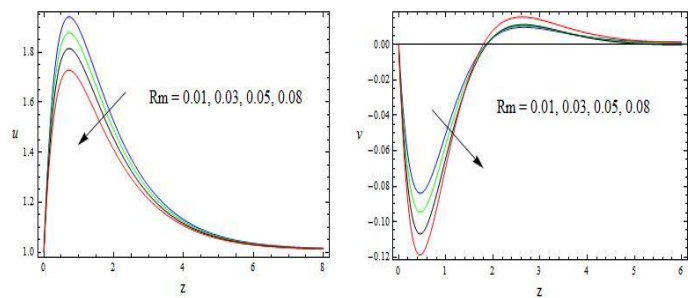
The rate of mass transfer ( $Sh$ ) is shown in the Table (3). The magnitude of the Sherwood number enhances throughout the fluid region with increasing scalar constant  $\mathcal{E}$ , suction velocity  $A$ , Schmidt number  $Sc$ , and the frequency of oscillation  $n$ .



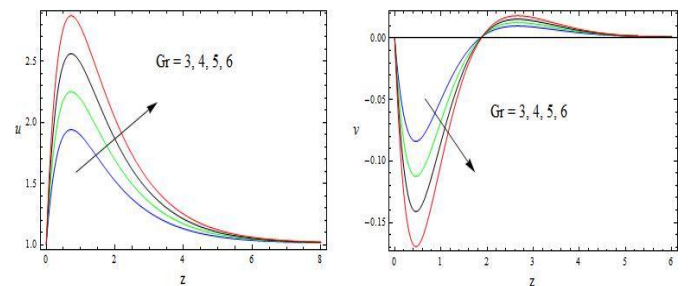
**Figures 2.** The velocity Profiles for  $u$  and  $v$  against  $M$   
 $\mathcal{E} = 0.01, n = 0.5, A = 0.5, K = 0.5, Gr = 3, Q = 0.1, Rm = 0.01, Pr = 0.71$



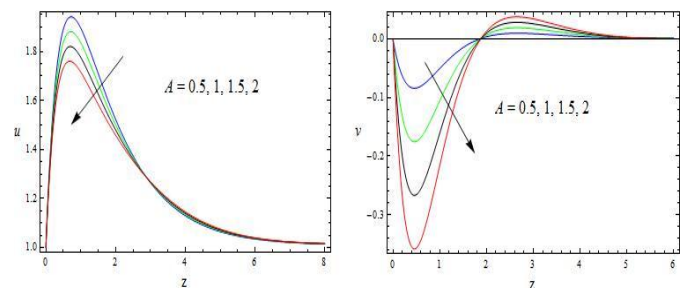
**Figures 3.** The velocity Profiles for  $u$  and  $v$  against  $K$   
 $M = 0.5, \mathcal{E} = 0.01, n = 0.5, A = 0.5, Gr = 3, Q = 0.1, Rm = 0.01, Pr = 0.71$



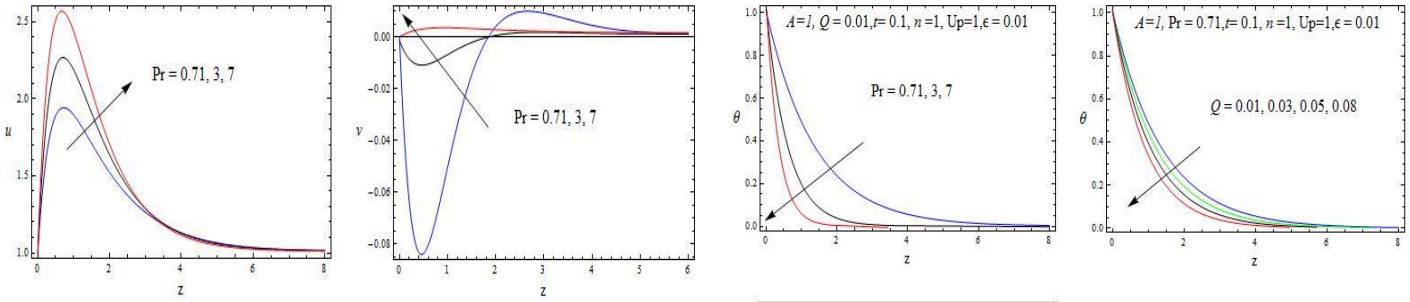
**Figures 4.** The velocity Profiles for  $u$  and  $v$  against  $R_m$   
 $M = 0.5, \mathcal{E} = 0.01, n = 0.5, A = 0.5, K = 0.5, Gr = 3, Q = 0.1, Pr = 0.71$



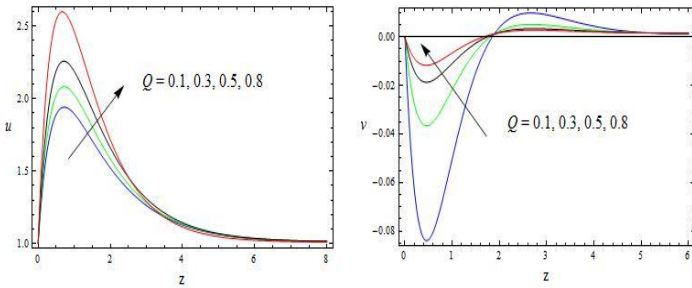
**Figures 5.** The velocity Profiles for  $u$  and  $v$  against  $Gr$   
 $M = 0.5, \mathcal{E} = 0.01, n = 0.5, A = 0.5, K = 0.5, Q = 0.1, Rm = 0.01, Pr = 0.71$



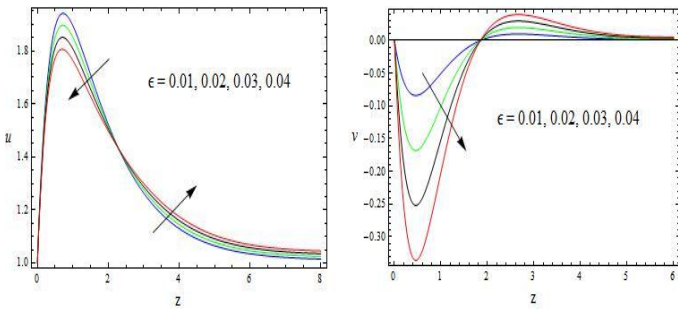
**Figures 6.** The velocity Profiles for  $u$  and  $v$  against  $A$   
 $M = 0.5, \mathcal{E} = 0.01, n = 0.5, K = 0.5, Gr = 3, Q = 0.1, Rm = 0.01, Pr = 0.71$



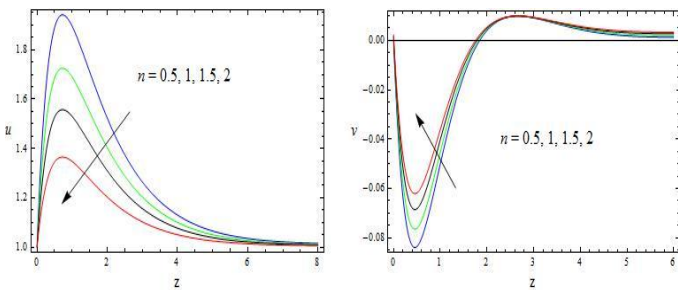
**Figures 7.** The velocity Profiles for  $u$  and  $v$  against  $Pr$   
 $M = 0.5, \epsilon = 0.01, A = 0.5, K = 0.5, n = 0.5, Gr = 3, Q = 0.1, Rm = 0.01$



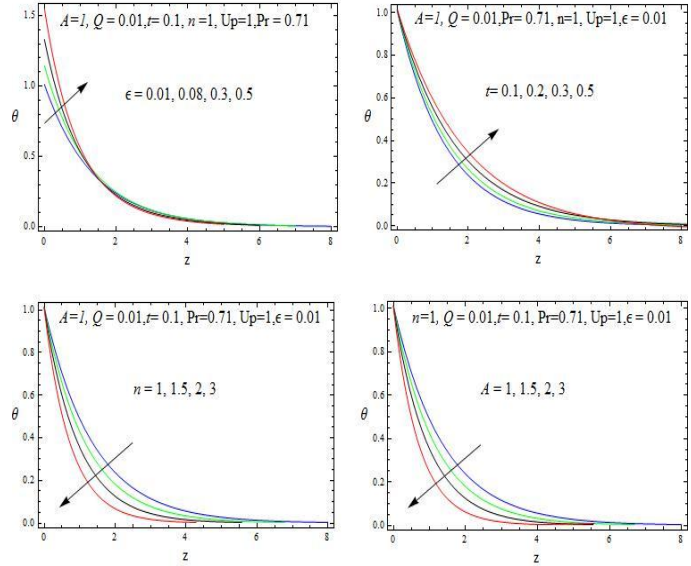
**Figures 8.** The velocity Profiles for  $u$  and  $v$  against  $Q$   
 $M = 0.5, \epsilon = 0.01, n = 0.5, A = 0.5, K = 0.5, Gr = 3, Rm = 0.01, Pr = 0.71$



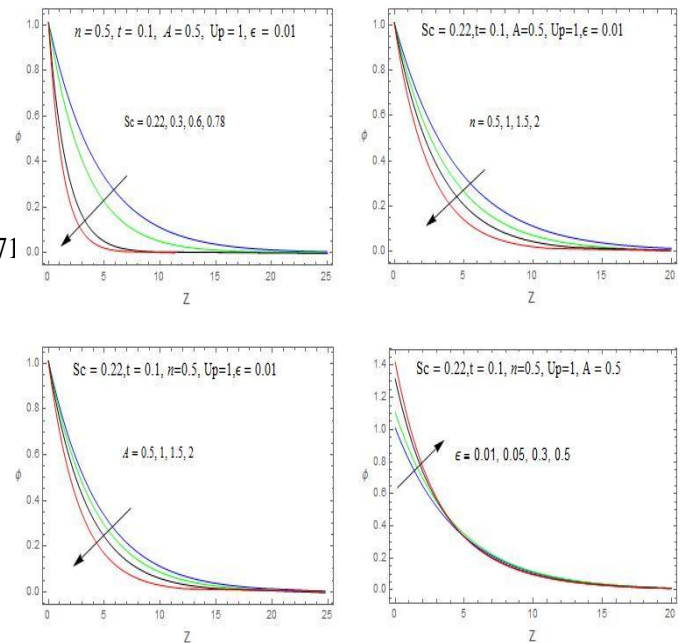
**Figures 9.** The velocity Profiles for  $u$  and  $v$  against  $\epsilon$   
 $M = 0.5, n = 0.5, A = 0.5, K = 0.5, Gr = 3, Q = 0.1, Rm = 0.01, Pr = 0.71$



**Figures 10.** The velocity Profiles for  $u$  and  $v$  against  $n$   
 $M = 0.5, \epsilon = 0.01, A = 0.5, K = 0.5, Gr = 3, Q = 0.1, Rm = 0.01, Pr = 0.71$



**Figures 11.** Temperature Profiles for  $\theta$  against  $Pr, Q, \epsilon, t, n$  and  $A$



**Figures 12.** Concentration Profiles for  $\phi$  against  $Sc, \epsilon, n$  and  $A$

**Table 1:** Skin friction coefficient

$M$	$K$	$Gr$	$R_m$	$A$	$Pr$	$Sc$	$Q$	$\varepsilon$	$n$	$\tau_x$	$\tau_y$
<b>0.5</b>	<b>0.5</b>	<b>3</b>	<b>0.01</b>	<b>0.5</b>	<b>0.71</b>	<b>0.22</b>	<b>0.1</b>	<b>0.01</b>	<b>0.5</b>	3.85552	-0.038415
<b>1</b>										2.91145	-0.032145
<b>2</b>										2.09855	-0.023144
	<b>1</b>									5.17965	-0.035896
	<b>1.5</b>									7.16021	-0.011774
		<b>4</b>								5.13415	-0.051748
		<b>5</b>								6.41965	-0.064855
			<b>0.03</b>							3.82552	-0.038965
			<b>0.05</b>							3.78748	-0.039854
				<b>1</b>						3.81854	-0.013785
				<b>1.5</b>						3.76585	0.010585
					<b>3</b>					2.14478	0.049855
					<b>7</b>					0.64854	0.050855
						0.3				3.55226	-0.038596
						0.6				3.25411	-0.035222
							<b>0.3</b>			5.34115	-0.065968
							<b>0.5</b>			9.16285	-0.070025
								<b>0.03</b>		3.95226	-0.114658
								<b>0.05</b>		4.01748	-0.190965
									<b>1</b>	3.81966	-0.042744
									<b>1.5</b>	2.57854	-0.094855

**Table 2:** Nusselt number (Nu)

$\varepsilon$	$A$	$Pr$	$Q$	$n$	Nu
<b>0.01</b>	<b>0.5</b>	<b>0.71</b>	<b>0.01</b>	<b>0.5</b>	-0.733466
<b>0.03</b>					-0.760672
<b>0.05</b>					-0.787877
	<b>1</b>				-0.735992
	<b>1.5</b>				-0.738518
		<b>3</b>			-3.059900
		<b>7</b>			-7.123040
			<b>0.03</b>		-0.752536
			<b>0.05</b>		-0.770710
				<b>1</b>	-0.736135
				<b>1.5</b>	-0.738739

**Table 3:** Sherwood number (Sh)

$\varepsilon$	$A$	$Sc$	$n$	Sh
<b>0.01</b>	<b>0.5</b>	<b>0.22</b>	<b>0.5</b>	-0.225384
<b>0.03</b>				-0.236151
<b>0.05</b>				-0.246918
	<b>1</b>			-0.225937
	<b>1.5</b>			-0.226491
		<b>0.3</b>		-0.306780
		0.6		-0.611766
			<b>1</b>	-0.226992
			<b>1.5</b>	-0.228478

## CONCLUSIONS

1. When scalar constant  $\mathcal{E}$  increase the velocity increase, whereas when dimensionless visco-elasticity parameter of the Rivlin–Ericksen fluid  $R_m$  and dimensionless heat absorption coefficient  $Q$ , increase the velocity decreases.
2. Heat absorption coefficient  $Q$  increase results a decrease in temperature but, a reverse case is noticed in the presence of a constant  $\mathcal{E}$ .
3. It is recognized that there are many other methods that could be considered in order to describe some reasonable solution for this particular type of problem.
4. For better understanding of the thermal and concentration behavior of this work, however, it may be necessary to perform the experimental works.

## REFERENCES

- [1]. Soundalgekar, V.M. and Puri, P. (1969) On Fluctuating Flow of an Elastic-Viscous Fluid past an Infinite Plate with Variable Suction. *Journal of Fluid Mechanics*, 35, 561-573.
- [2]. Shen, F., Tan, W., Zhao, Y. and Masuoka, T. (2006) The Rayleigh-Stokes Problem for a Heated Generalized Second Grade Fluid with Fractional Derivative Model. *Nonlinear Analysis: Real World Applications*, 7, 1072-1080.
- [3]. Varshney, C.L. (1979) Fluctuating Flow of Viscous Fluid through a Porous Medium Bounded by a Porous Plate. *Indian Journal of Pure and Applied Mathematics*, 10, 1558-1564.
- [4]. Lighthill, M.J. (1954) The Response of Laminar Skin Friction and Heat Transfer to Fluctuations in the Stream Velocity. *Proceedings of the Royal Society A*, 224, 1-23.
- [5]. Messiha, S.A.S. (1966) Laminar Boundary Layer in Oscillating Flow along an Infinite Flat Plate with Variable Suction. *Proceedings of the Cambridge Philosophical Society*, 62, 329-337.
- [6]. Stuart, J.T. (1955) A Solution of the Navier-Stokes and Energy Equations Illustrating the Response of Skin Friction and Temperature of an Infinite Plate Thermometer to Fluctuations in the Stream Velocity. *Proceedings of the Royal Society A*, 231, 116-130.
- [7]. Gholizadeh, A. (1990) MHD Oscillatory Flow past a Vertical Porous Plate through Porous Medium in the Presence of Thermal and Mass Diffusion with Constant Heat Source. *Astrophysics and Space Science*, 174, 303-310.
- [8]. Moniem, A.A. and Hassanin, W.S. (2013) Solution of MHD Flow past a Vertical Porous Plate through a Porous Medium under Oscillatory Suction. *Applied Mathematics*, 4, 694-702.
- [9]. Venkateswarlu, M., Ramana Reddy, G.V. and Lakshmi, D.V. (2013) Unsteady MHD Flow of a Viscous Fluid past a Vertical Porous Plate under Oscillatory Suction Velocity. *Advances in Applied Science Research*, 4, 52-67.
- [10]. Raghunath, Siva prasad and GSS Raju (2018) Heat and mass transfer on Unsteady MHD flow of a second grade fluid through porous medium between two vertical plates, *JUSPS-B Vol. 30(2)*, 1-11 (2018).
- [11]. Soundalgekar, V.M. and Takhar, H.S. (1977) MHD Oscillatory Flow past a Semi Infinite Plate. *AIAA Journal*, 15, 457-458.
- [12]. VeeraKrishna.M and B.V.Swarnalathamma (2016) Convective Heat and Mass Transfer on MHD Peristaltic Flow of Williamson Fluid with the Effect of Inclined Magnetic Field,” *AIP Conference Proceedings* 1728:020461
- [13]. Swarnalathamma. B. V. and M. Veera Krishna (2016) Peristaltic hemodynamic flow of couple stress fluid through a porous medium under the influence of magnetic field with slip effect *AIP Conference Proceedings* 1728:020603
- [14]. VeeraKrishna.M and M.Gangadhar Reddy (2016) MHD free convective rotating flow of Visco-elastic fluid past an infinite vertical oscillating porous plate with chemical reaction *IOP Conf. Series: Materials Science and Engineering* 149:012217
- [15]. K. Raghunath, M. Veera Krishna (2016) Heat and Mass Transfer on Unsteady MHD Flow of a Visco-Elastic Fluid Past an Infinite Vertical Oscillating Porous Plate, *British Journal of Mathematics & Computer Science* 17(6): 1-18, 2016, Article no.BJMCS.25872